Mineralogical Magazine, June 2014, Vol. 78(3), pp. 757–774

Arsenic-bearing new mineral species from Valletta mine, Maira Valley, Piedmont, Italy: I. Grandaite, $Sr_2Al(AsO_4)_2(OH)$, description and crystal structure

F. Cámara[1,2,*], M. E. Ciriotti[3], E. Bittarello[1,2], F. Nestola[4], F. Massimi[5], F. Radica[6], E. Costa[1], P. Benna[1,2] and G. C. Piccoli[7]

[1] Dipartimento di Scienze della Terra, Università degli Studi di Torino, via Valperga Caluso 35, I-10125 Turin, Italy
[2] CrisDi, Interdepartmental Center for Crystallography, via Pietro Giuria 7, I-10125, Turin, Italy
[3] Associazione Micromineralogica Italiana, via San Pietro 55, I-10073 Devesi-Cirié, Turin, Italy
[4] Dipartimento di Geoscienze, Università degli Studi di Padova, via G. Gradenigo 6, I-35131 Padua, Italy
[5] Dipartimento di Ingegneria Meccanica e Industriale, Università degli Studi Roma Tre, via della Vasca Navale 79, I-00146 Rome, Italy
[6] Dipartimento di Scienze Geologiche, Università degli Studi Roma Tre, largo San Leonardo Murialdo 1, I-00146 Rome, Italy
[7] Amici del Museo "F. Eusebio", via Paruzza 1, I-12051 Alba, Italy

[*Received 19 January 2014; Accepted 27 February 2014; Associate Editor: A. Christy*]

ABSTRACT

The new mineral species grandaite, ideally $Sr_2Al(AsO_4)_2(OH)$, has been discovered on the dump of Valletta mine, Maira Valley, Cuneo province, Piedmont, Italy. Its origin is related to the reaction between the ore minerals and hydrothermal solutions. It occurs in thin masses of bright orange to salmon to brown coloured crystals, or infrequently as fan-like aggregates of small (<1 mm) crystals, with reddish-brown streak and waxy to vitreous lustre. Grandaite is associated with aegirine, baryte, braunite, hematite, tilasite, quartz, unidentified Mn oxides and Mn silicates under study.

Grandaite is biaxial (+) with refractive indices α = 1.726(1), β = 1.731(1), γ = 1.752(1). Its calculated density is 4.378 g/cm^3. Grandaite is monoclinic, space group $P2_1/m$, with a = 7.5764(5), b = 5.9507(4), c = 8.8050(6) Å, β = 112.551(2)º, V = 366.62(4) Å^3 and Z = 2. The eight strongest diffraction lines of the observed X-ray powder diffraction pattern are [d in Å, (I), (hkl)]: 3.194 (100)($\bar{2}$11), 2.981 (50.9)(020), 2.922 (40.2)($\bar{1}$03), 2.743 (31.4)(120), 2.705 (65.2)(112), 2.087 (51.8) ($\bar{1}$23), 1.685 (24.5)(321), 1.663 (27.7)(132). Chemical analyses by electron microprobe gave (wt.%) SrO 29.81, CaO 7.28, BaO 1.56, Al_2O_3 7.07, Fe_2O_3 2.34, Mn_2O_3 1.88, MgO 1.04, PbO 0.43, As_2O_5 44.95, V_2O_5 0.50, P_2O_5 0.09, sum 96.95; H_2O 1.83 wt.% was calculated by stoichiometry from the results of the crystal-structure analysis. Raman and infrared spectroscopies confirmed the presence of $(AsO_4)^{3-}$ and OH groups. The empirical formula calculated on the basis of 9 O a.p.f.u., in agreement with the structural results, is $(Sr_{1.41}Ca_{0.64}Ba_{0.05}Pb_{0.01})_{\Sigma=2.11}(Al_{0.68}Fe^{3+}_{0.14}Mn^{3+}_{0.12}Mg_{0.13})_{\Sigma=1.07}$ $[(As_{0.96}V_{0.01})_{\Sigma=0.97}O_4]_2(OH)$, the simplified formula is $(Sr,Ca)_2(Al,Fe^{3+})(AsO_4)_2(OH)$ and the ideal formula is $Sr_2Al(AsO_4)_2(OH)$.

The crystal structure was solved by direct methods and found to be topologically identical to that of arsenbrackebuschite. The structure model was refined on the basis of 1442 observed reflections to R_1 = 2.78%. In the structure of grandaite, chains of edge-sharing M^{3+} octahedra run along [010] and share vertices with T^{5+} tetrahedra, building up $[M^{3+}(T^{5+}O_4)_2(OH, H_2O)]$ units, which are connected through

* E-mail: fernando.camaraartigas@unito.it
DOI: 10.1180/minmag.2014.078.3.21

interstitial divalent cations. Grandaite is named after the informal appellation of the province where the type locality is located. The new mineral was approved by the International Mineralogical Association Commission on New Minerals, Nomenclature and Classification (IMA2013-059). The discovery of grandaite and of other members of the group (description still in progress) opens up the possibility of exploring the crystal chemistry of the brackebuschite supergroup.

Keywords: grandaite, arsenate, arsenbrackebuschite group, new mineral species, crystal structure, Valletta, Piedmont, Italy.

Introduction

Arsenic is not a very abundant element. It accounts for ~1.5 ppm of the Earth's crust, making it the 47th most abundant element (Vaughan, 2006). On average, soils contain 1–10 ppm of As, while seawater has only 1.6 ppb As (Emsley, 2011). In its most common natural form, As occurs as colourless, odourless, crystalline As_2O_3 (the lethal 'white arsenic' corresponding to both arsenolite and claudetite) and As_2O_5, which are hygroscopic and readily soluble in water forming acidic solutions. Arsenic acid (containing As^{5+}), $AsO(OH)_3$, is a weak acid, which forms arsenates responsible for As contamination of groundwater, a problem that affects many people (e.g. Mukherjee *et al.*, 2006; Twarakavi and Kaluarachchi, 2006), making the geochemical investigation of As very important.

In some respects As compounds resemble those of P (another Group V element). The protonation steps between the arsenate and As acid are similar to those between phosphate and phosphoric acid. The most common oxidation states for As are: −3 in the arsenides (such as alloy-like intermetallic compounds), +3 in the arsenites and +5 in the arsenates and most organoarsenic compounds. Arsenic also bonds to itself readily as seen for example in the square As_4^{3-} ions in the mineral skutterudite. In oxides, As^{+3} occurs typically as a pyramidal AsO_3 group in which all oxygens lie to one side of the As^{+3} ion due to a stereoactive lone pair of electrons (Norman, 1998), while in the +5 oxidation state it is typically coordinated tetrahedrally.

To date >260 arsenates, <30 arsenites and <10 silicoarsenates are recognized as valid mineral species by the Commission on New Minerals, Nomenclature and Classification (CNMNC) of the International Mineralogical Association (IMA). The recognition of new arsenate mineral species at the Valletta mine dumps (Piedmont, Italy) make this a significant mineralogical locality. Grandaite (IMA2013-059) represents the third Sr-dominant arsenate of the mineral species recognized as valid by IMA-CNMNC, after arsenogoyazite, $SrAl_3(AsO_4)(AsO_3OH)(OH)_6$ (Walenta and Dunn, 1984) and kemmlitzite, $SrAl_3(AsO_4)(SO_4)(OH)_6$ (Hak *et al.*, 1969). The new mineral species strontiopharmacosiderite, $Sr_{0.5}Fe_4^{3+}(AsO_4)_3(OH)_4{\cdot}4H_2O$ (pers. comm. S. J. Mills, 2013) was approved after grandaite (IMA2013-101).

This is the first of a series of formal descriptions of new As-bearing minerals from the Valletta mine. Samples containing grandaite were collected by one of the authors (GCP) in 2001 and later in 2009 on the dumps of the Valletta mine, Valletta Valley ('Vallone della Valletta' in Italian), Canosio municipality, Maira Valley, Cuneo province, Piedmont, Italy (44º23′42″N, 7º5′42″E, 2536 m asl). The Valletta mine is a small Fe-Mn-As deposit that has never been studied geologically or petrologically. The name of grandaite is for the informal appellation of the Province where the type locality (Valletta mine) is located. The Cuneo Province is popularly and historically called "la Granda" (the Big One) for its considerable extent, mostly in the Alpine region (Maritime and Cottian Alps south of Mount Monviso). At 6903 km^2 it is one of the biggest in Italy.

A fragment of holotype material is deposited in the mineralogical collection of the Museo Regionale di Scienze Naturali di Torino, Sezione di Mineralogia, Petrografia e Geologia, via Giovanni Giolitti 36, I–10123 Torino, Italy, catalogue number M/15999 and another in the mineralogical collection of the Museo Civico Archeologico e di Scienze Naturali "Federico Eusebio", via Vittorio Emanuele 19, I–12051 Alba, Cuneo, Italy, catalogue number G. 1723 prog. 505.

Not long after submitting the manuscript our good friend and colleague Bruno Lombardo passed away. He very much loved the Alps and has devoted much effort to the mineralogy of Piedmont, contributing passionately to the

exploration and knowledge of many mineralogical localities. We dedicate this paper to his memory.

Geological setting and mineral occurrence

The Valletta Fe-Mn deposit is located in the Briançonnais Zone of the Cottian Alps. Specifically, the Mn minerals are hosted in Permian quartzites overlying quartzose conglomerates of the Verrucano facies and quartz-feldspar fine-grained schists derived from Permian rhyolitic volcanism of the so-called Axial Permian–Carboniferous Zone (Franchi and Stella, 1930). A major subvertical tectonic contact, Faille de Ceillac (Gidon *et al.*, 1994) separates the rocks found at Valletta mine from the Middle Triassic carbonate sequence of the Becco Grande to the north and from the Rocca La Meja ridge to the south. The rocks found at Valletta mine are part of the Bande de Marinet, the southernmost tectonic zone of the Axial Permian–Carboniferous Zone; specifically it is part of Unit M3, the structurally highest unit defined in the Bande de Marinet by Lefèvre (1982). During the Alpine tectonometamorphic cycle the rocks now exposed in the Bande de Marinet were subjected to high-*P*, low-*T* metamorphism of blueschist facies, the effects of which are more evident in the metabasites intercalated in the metavolcanic quartz-feldspar schists that often display the characteristic lawsonite-glaucophane assemblage (Franchi and Stella, 1930; Gidon *et al.*, 1994). Grandaite is probably the result of crystallization from hydrothermal fluids in an oxidizing environment (the occurrence of hematite, braunite and arsenates agree with this hypothesis); arsenic could be derived from the surrounding Fe-Mn ores, as observed by several authors in other small hydrothermal Fe-Mn deposits from the Alps (e.g. Brugger and Gieré, 1999).

A brief mineralogical note on the Valletta mine was given by Piccoli (2002). During the first exploration, the remains of an old mining operation, probably an open pit, were found at the head of the Valletta Valley, near Canosio, in the Maira Valley (Cuneo, Piedmont, Italy). Historical information on a mine active in 1455 in the Saluzzo Marquisate (of which Canosio was part) are summarized by Mangione (1999) and Pipino (2010). The translation of the historical medieval text is as follows: "*September 10, 1455: Perpetual lease made by the Marquis Ludovico di Saluzzo to Antonio Petro, late Petrino, and Antonio Bordello, alias Poncetto, of a small assay of an iron mine in the territory of Canosio, at the Valletta, with 12 fathoms of land not so far, by the tithe of the ore.*"

However, the deposit has never been studied from a genetic point of view and available geological data for the area studied are very limited. Other than the historic text reported above, there is no mention in the literature of the occurrence of ore mineralization. Preliminary work carried out during sampling of grandaite showed that it is a small Fe-(Mn) deposit enriched in As. Grandaite-bearing quartz veins are hosted within compact, granular, dark red (verging on black) quartzite. Blocks of this material have been dug and piled up in a small landfill where they are mixed with calcareous rocks, also from the excavated material.

The new mineral is strictly associated with aegirine, adelite $CaMg(AsO_4)(OH)$, baryte, braunite, hematite, quartz, tilasite $CaMg(AsO_4)F$, unidentified Mn oxides and Mn silicates under study.

In addition to grandaite, a number of other As-rich mineral species occur in this small dump, some of them are currently under study. These findings make the small dump of the Valletta mine a reference locality for the study of arsenate and silicoarsenate mineral species, similar to those of the Graveglia Valley, Liguria, Italy (Antofilli *et al.*, 1983; Borgo and Palenzona, 1988; Palenzona, 1991, 1996). Other As-rich minerals found in the rock samples collected in the dump, although not strictly associated with grandaite are: the arseniopleite–caryinite series $(Ca,Na)NaMn^{2+}(Mn^{2+},Mg,Fe^{2+})_2(AsO_4)_3$ – $(Na,Pb)(Ca,Na)CaMn_2^{2+}(AsO_4)_3$, azurite, berzeliite $NaCa_2Mg_2(AsO_4)_3$, manganberzeliite $NaCa_2Mn_2^{2+}(AsO_4)_3$, tiragalloite $Mn_4^{2+}As^{5+}Si_3O_{12}(OH)$, braccoite (IMA 2013-093) $NaMn_5^{2+}[Si_5As^{5+}O_{17}(OH)](OH)$; these are found along with albite, calcite, diopside, ganophyllite, ilmenite, hollandite, malachite, magnesio-riebeckite, magnetite, Mn-bearing muscovite, orthoclase, rutile, rhodonite and titanite.

Mineralogical characterization

Appearance and physical properties

Grandaite occurs as subhedral crystals in thin masses, a few cm in size, with uneven fracture (Fig. 1), or infrequently as fan-like aggregates of small crystals, in white veins of compact quartz

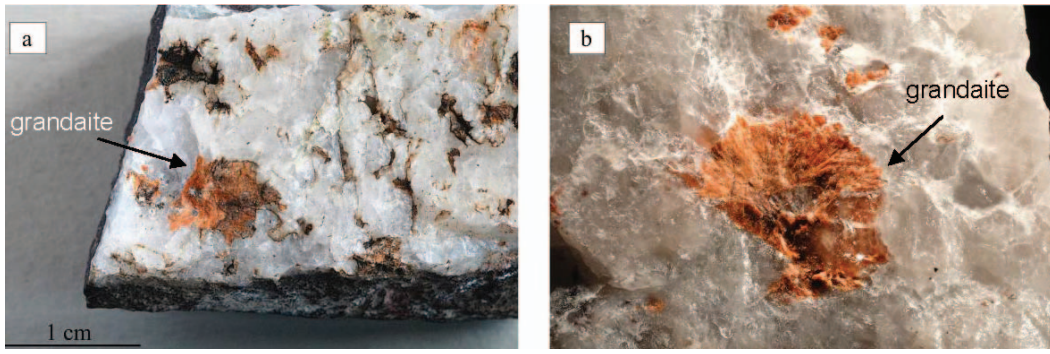

FIG. 1. Images of grandaite: (a) the holotype specimen deposited in the Museo Regionale di Scienze Naturali di Torino and (b) a fan-like aggregate (~1 cm × 1 cm) of grandaite in a quartz matrix, from the collection of G.C. Piccoli. Photo G.C. Piccoli.

on reddish-brownish-black K-feldspar crossing, in a disorganized manner, the granular red-brown quartzite. Well-formed crystals, typically platy tablets, are very rare and are rarely included in more hyaline quartz and/or the blackish matrix on fracture surfaces.

Individual crystals are bright orange to salmon to brown and no twinning is observed. Grandaite is translucent and has a reddish-brown streak, a waxy to vitreous lustre and does not fluoresce under SW or LW ultraviolet light. Grandaite is optically biaxial (+), with 2V(meas.) = 52(2)º and 2V(calc.) = 53º. The measured refractive indices are α = 1.726(1), β = 1.731(1), γ = 1.752(1) (589 nm).

The mineral is brittle. No cleavage or parting is observed. Hardness was measured by nano-indentation by using an Agilent Nano Indenter G200 at the Università di Roma Tre – LIME performed in CSM (continuous stiffness measurement) mode, with a frequency of 45 Hz, amplitude of oscillation 2 nm, constant strain rate of 0.05 s^{-1} and a maximum penetration depth of 1000 nm. Results of hardness and modulus profiles were obtained after averaging >25 different tests. The instrument was completely re-calibrated before testing by performing a series of indentations on a certified amorphous silica reference sample. Observed elastic modulus is 121.9 ± 11 GPa (displacement 90–110 nm) and hardness, H = 9.95 ± 1.29 GPa (displacement 90–110 nm); Vickers Hardness was calculated from H in order to determine Mohs hardness, resulting in a Mohs hardness of 6–6½. It is not practicable to provide actual Vickers hardness units because the method for obtaining hardness used a continuous variation of the load. Density was not measured due to the small crystal size and its intergrowths with adelite and baryte. The calculated density obtained from the empirical formula and unit-cell parameters measured during the single-crystal study is 4.378 g/cm^3.

Chemical data

The chemical composition of grandaite was determined using a Cameca SX-50 electron microprobe (wavelength-dispersive spectroscopy (WDS) mode) at the Dipartimento di Geoscienze (Università di Padova) on a thin section sampled from the holotype close to the place where the crystal used for the diffraction study was extracted. Major and minor elements were determined at 20 kV accelerating voltage and 20 nA beam current (beam size = 2 μm), with 40 to 20 s counting time on both peak and background. X-ray counts were converted to oxide wt.% using the *PAP* correction program supplied by Cameca (Pouchou and Pichoir, 1984, 1985).

The crystals studied in the thin section (Fig. 2) were found to be homogeneous. On the basis of preliminary quantitative scanning electron microscopy (using energy-dispersive spectroscopy) using a Cambridge S-360 microscope equipped with an Oxford INCA Energy 200 (with ultrathin window) at the Dipartimento di Scienze della Terra (Università di Torino), analyses for Na, K, Y, *REE*, F and Cl were not performed in the present WDS study; Si, Nb, Ti, Ta and S were checked but were below detection limits. The results of eight analyses are given in Table 1.

The empirical formula, calculated on the basis of 9 O a.p.f.u. (atoms per formula unit), is, within rounding errors, $(Sr_{1.41}Ca_{0.64}Ba_{0.05}Pb_{0.01})_{\Sigma=2.11}$ $(Al_{0.68}Fe^{3+}_{0.14}Mn^{3+}_{0.12}Mg_{0.13})_{\Sigma=1.07}$

FIG. 2. Image of the thin section of the holotype showing grandaite in the marked area associated with a quartz vein, cutting a braunite-hematite-bearing quartzite. Plane-polarized light.

$[(As_{0.96}V_{0.01})_{\Sigma=0.97}O_4]_2(OH)$. The presence of OH was confirmed by Raman and Fourier-transform infrared spectroscopy (FTIR) (see next sections). Fe was considered as Fe^{3+} on the basis of site-bond length observed from structure refinement. The simplified formula is $Sr_2Al(AsO_4)_2(OH)$, which requires SrO 41.68, Al_2O_3 10.23, As_2O_5 46.28, H_2O 1.81, total 100.00 wt.%. The mean refractive index *n* of grandaite, the calculated density and the empirical formula yielded a Gladstone-Dale compatibility index (Mandarino, 1979, 1981) of 0.032 rated as excellent.

Grandaite is unreactive and insoluble in 2 M and 10% HCl and 65% HNO_3.

Micro-Raman spectroscopy

The Raman spectrum of grandaite (Fig. 3) was obtained at the Dipartimento di Scienze della Terra (Università di Torino) using a micro/macro Jobin Yvon Mod. LabRam HRVIS, equipped with a motorized *x–y* stage and an Olympus microscope. The backscatter Raman signal was collected with a 50× objective and the Raman spectrum was obtained for a non-oriented crystal. The 632.8 nm line of an He-Ne laser was used as excitation; laser power was controlled by means of a series of density filters. The minimum lateral and depth resolution were set to few μm. The system was calibrated using the 520.6 cm^{-1} Raman band of Si before each experimental session. The spectra were collected with 2–6 acquisitions and counting times ranging between 20 and 180 s. Spectral manipulation such as baseline adjustment, smoothing and normalization

TABLE 1. Analytical data for grandaite.

	Wt.%	Range	Std. dev.	Probe standard
SrO	29.81	28.51–30.57	0.64	celestine ($L\alpha$)
CaO	7.28	6.79–7.74	0.48	wollastonite ($K\alpha$)
BaO	1.56	0.79–2.63	0.56	baryte ($L\alpha$)
Al_2O_3	7.07	6.76–7.79	0.38	Al_2O_3 ($K\alpha$)
Fe_2O_3**	2.34	2.09–2.63	0.28	Fe_2O_3 ($K\alpha$)
Mn_2O_3	1.88	1.36–2.14	0.24	$MnTiO_3$ ($K\alpha$)
MgO	1.04	0.76–1.40	0.18	MgO ($K\alpha$)
PbO	0.43	0.16–0.55	0.13	Pb ($M\alpha$)
As_2O_5	44.95	44.48–45.71	0.46	GaAs ($L\alpha$)
V_2O_5	0.50	0.32–0.65	0.12	vanadinite ($K\alpha$)
P_2O_5	0.09	0.06–0.12	0.02	apatite ($K\alpha$)
H_2O*	1.83	1.82–1.86	0.01	
Total	98.78	98.23–99.18	0.30	

* Calculated by stoichiometry from the results of the crystal-structure analysis. **All Fe is considered as Fe^{3+} on the basis of structure-refinement results.
Std dev. = standard deviation

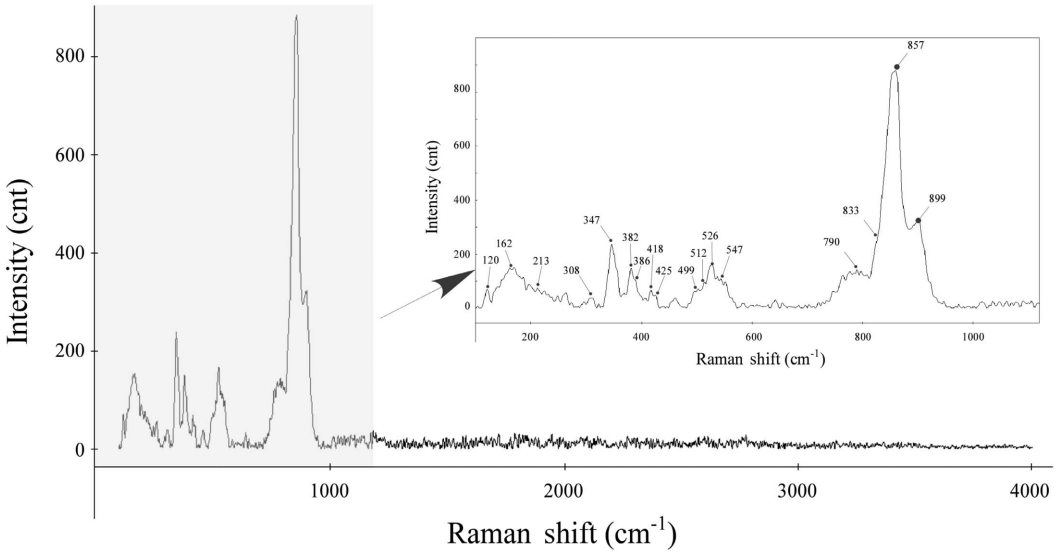

FIG. 3. Raman spectra of grandaite in the 200–4000 cm^{-1} region and between 200 and 1200 cm^{-1}.

were performed using the *LabSpec 5* software package (Horiba Jobin Yvon, 2004, 2005). Band-component analysis was undertaken using the *Fityk* software package (Wojdyr, 2010), which enabled the type of fitting function to be selected and allows specific parameters to be fixed or varied accordingly. The spectrum was recorded using the *LabSpec 5* program from 100 to 4000 cm^{-1} and the results of the spectroscopic analysis are reported below.

Bands with frequencies between 200 and 600 cm^{-1} correspond to As^{5+}–O bending vibrations, while bands lower than 200 cm^{-1} correspond to lattice modes (120, 162, 213 cm^{-1}).

In detail, multiple Raman bands are observed at 308, 347, 382, 386, 418, 425 cm^{-1}. The first two bands are assigned to the ν_2 $(AsO_4)^{3-}$ symmetric bending vibration (E) and the latter four bands are assigned to the ν_4 bending vibration (F2). The assignment of these bands is in harmony with the analysis of arsenate vibrations according to Myneni *et al.* (1998*a*,*b*) and Nakamoto (1986). A broad band centred upon 500 cm^{-1}, which may be resolved into component bands at 499, 512, 526 and 547 cm^{-1} probably includes bands attributable to the ν_4 $(AsO_4)^{3-}$ bending mode. The observation of multiple bands is characteristic of the reduced symmetry of the AsO_4 unit in the crystal (Frost and Keeffe, 2011). In the range 700–950 cm^{-1} the spectra are complex, showing multiple bands that can be attributed to As^{5+}–O stretching vibrations of AsO_4^{3-} groups. A broad envelope of overlapping bands centred on 858 cm^{-1} can be resolved with band-component analysis to show two intense bands at 857 and 833 cm^{-1}. These bands are assigned to the ν_1 $(AsO_4)^{3-}$ symmetrical stretching and ν_3 $(AsO_4)^{3-}$ antisymmetrical stretching modes. Other bands are found at 899 and 790 cm^{-1} which may also be ascribed to the ν_3 $(AsO_4)^{3-}$ antisymmetrical stretching mode or may be attributed to the hydroxyl deformation mode (Frost and Keeffe, 2011). The absence of strong bands with frequencies >950 cm^{-1} indicates the absence of H-, C-, N- and B-bearing groups in grandaite, but in the region between 2500 and 4000 cm^{-1} (hydroxyl stretching region) the spectrum displays a considerable amount of noise and this is a result of the low intensity of the bands. Due to this, the presence of some measurable OH content could not be excluded so the infrared spectrum of grandaite was collected.

Infrared spectroscopy

Infrared (IR) spectra (Fig. 4) were collected at the Università di Roma Tre using a Bruker Hyperion 3000 IR-microscope equipped with a liquid nitrogen-cooled MCT detector. The powder spectrum was collected with a Bruker Optics VERTEX 70v FTIR spectrometer equipped with a KBr beamsplitter, a DTGS detector and a

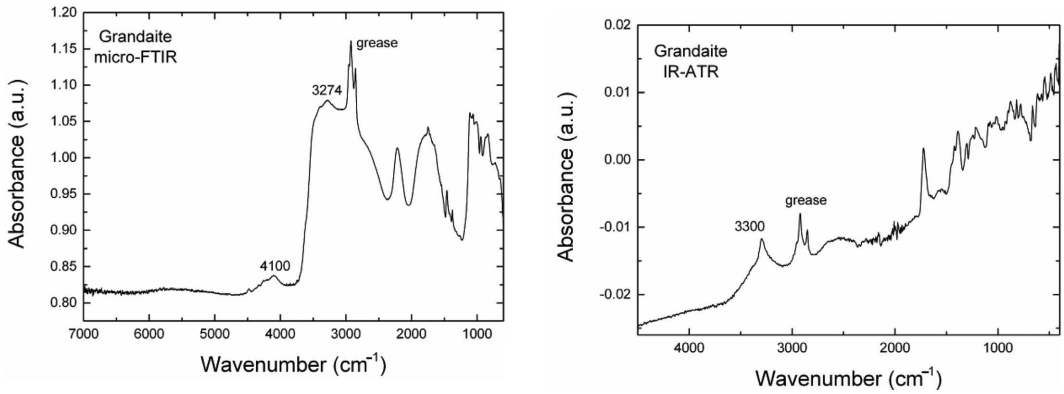

FIG. 4. Infrared spectra: (*left*) single-crystal infrared spectrum; (*right*) powder spectrum collected with a MIRacle Diamond ATR accessory.

MIRacle Diamond ATR accessory. For both, the nominal resolution was 4 cm^{-1} and 128 scans were averaged for background and sample. Infrared confirmed the presence of H (absorption band at ~3300 cm^{-1}) as hydroxyl showing strong H bonding. Using the Libowitzky (1999) correlation a frequency of 3200 cm^{-1} yields d(O···O) = 2.70 Å and d(H···O) = 1.85 Å. The presence of an absorption band at ~4100 cm^{-1} in the μ-IR spectrum can be assigned to a combination of stretching and bending modes of (OH) groups, although they could be also assigned to hypertones or combinations related to the $(AsO_4)^{3-}$ group.

X-ray diffraction

The powder X-ray diffraction pattern of grandaite was obtained at CrisDi (Università di Torino) using an Oxford Gemini R Ultra diffractometer equipped with a CCD area detector, with graphite-monochromatized Mo$K\alpha$ radiation. Indexing of reflections was based on a calculated powder pattern obtained by the structural model, using the software *PLATON v–140513* (Spek, 2009). Experimental and calculated data are reported in Table 2.

The unit-cell parameters refined from the powder data with the software *GSAS* (Larson and Von Dreele, 1994) are a = 7.575(1), b = 5.9526(9), c = 8.765(2) Å, β = 112.55(2)º and V = 366.62(4) $Å^3$.

Single-crystal X-ray diffraction data were collected using a Bruker AXS SMART APEX diffractometer with a CCD detector (Mo$K\alpha$ radiation) at Università di Pavia (Pavia, Italy). A crystal fragment showing sharp optical extinction behaviour was used for collecting intensity data. Crystal data and experimental details are reported in Table 3. The intensities of 6095 reflections with $-12 < h < 12$, $-9 < k < 9$ and $-14 < l < 14$ were collected up to 69.9º2θ using 0.2º frame and an integration time of 10 s. Data were integrated and corrected for Lorentz and polarization background effects, using the package *SAINT V6.45A* (Bruker AXS, 2003). Data were corrected using the empirical absorption correction (*SADABS*, Sheldrick, 2008). Refinement of the unit-cell parameters was based on 2404 measured reflections with $I > 10\sigma(I)$. At room temperature, the unit-cell parameters are a = 7.5764(5), b = 5.9507(4), c = 8.8050(6) Å, β = 112.551(2)º, V = 366.62(4) $Å^3$, space group $P2_1/m$, Z = 2. The a:b:c ratio is 1.273:1:1.480. A total of 1734 independent reflections were collected and the structure was solved and refined by means of the *SHELX* set of programs (Sheldrick, 2008).

Description of the structure

Structure model

The structure was refined starting from the atom coordinates of arsenbrackebuschite (Hofmeister and Tillmanns, 1978). Site-scattering values were refined for the cation sites using two scattering curves contributing proportionally and with a sum constrained to full occupancy: As and V were used for the sites T(1) and T(2); Al and Fe were considered for the M site; Sr and Ca were used for the A(1) site; and Sr and Ba for the A(2) site. A peak of ~2.7 e.$Å^{-3}$ was found in the difference-Fourier map, close to the A(2) site (~0.7 Å) and it

TABLE 2. X-ray powder diffraction data for grandaite. The eight strongest reflections are reported in bold*.

h	k	l	d_{obs} (Å)	d_{calc} (Å)	I_{rel}	I_{calc}
0	0	1		8.131		10.9
0	0	2		4.066		9.3
1	1	1		3.597		11.7
2	0	0		3.499		12.5
0	1	2		3.357		6.3
$\bar{2}$	**1**	**1**	**3.194**	**3.193**	**100.00**	**100.0**
0	**2**	**0**	**2.981**	**2.975**	**50.93**	**83.0**
$\bar{1}$	**0**	**3**	**2.922**	**2.935**	**40.20**	**80.4**
$\bar{2}$	1	2		2.930		11.6
2	0	1		2.842		14.2
0	2	1	2.798	2.794	6.55	8.2
1	**2**	**0**	**2.743**		**31.39**	
1	**1**	**2**	**2.705**	**2.710**	**65.19**	**61.0**
2	1	1	2.563	2.565	5.02	9.7
1	2	1	2.486	2.485	21.13	10.8
$\bar{2}$	1	3	2.455	2.461	16.05	9.3
0	2	2	2.400		7.45	
$\bar{3}$	1	1	2.315		12.81	
3	0	0		2.332		7.2
$\bar{2}$	0	4	2.144	2.153	8.04	11.9
1	2	2	2.127		11.19	
2	1	2	2.108		5.38	
$\bar{1}$	**2**	**3**	**2.087**	**2.089**	**51.75**	**29.5**
$\bar{1}$	1	4	2.047		7.05	
3	0	1		2.044		18.0
$\bar{2}$	1	4	2.017		5.55	
$\bar{2}$	2	3	1.999		5.56	
$\bar{4}$	0	2	1.891	1.892	10.70	22.8
$\bar{3}$	1	4	1.845	1.850	22.42	16.5
$\bar{4}$	0	3		1.822		8.9
$\bar{2}$	3	1	1.759		10.32	
$\bar{2}$	3	1		1.757		13.1
2	1	3	1.745		5.93	
4	0	0		1.749		6.0
3	**2**	**1**	**1.685**	**1.685**	**24.52**	**19.9**
1	**3**	**2**	**1.663**	**1.662**	**27.65**	**13.1**
$\bar{4}$	2	2	1.597	1.596	14.40	9.8

* Only reflections with $I_{rel} > 5\sigma(I_{rel})$ are listed.

was considered occupied by Pb. Due to the low occupancy (i.e. 0.03 a.p.f.u. of Pb) it was not added to the model. Another peak in the difference-Fourier map was found close to O(7) and added to the model as an H atom with fixed coordinates, an isotropic displacement factor of 0.02 Å^2 and full occupancy. Scattering curves for neutral atoms were taken from the International Tables for Crystallography (Wilson, 1992). Refinement converged to R_1 = 0.029 for 1442 observed reflections with $F_o > 4\sigma(F_o)$ and 84 parameters. Tables 4, 5 and 6 report: atom coordinates; displacement parameters; and selected bond distances and angles, respectively. Bond-valence calculations using the parameters of Brown (1981) are reported in Table 7. Tables of structure factors and a crystallographic information file (CIF) have been deposited with the Principal Editor of *Mineralogical Magazine* and are available from www.minersoc.org/pages/e_ journals/dep_mat_mm.html.

Site occupancies

Cation sites

The observed site scattering 15.40(3) e.p.s. (electrons per site) at the *M* site agrees well with the chemical data confirming an Al dominance at that site ($Al_{0.68}$ + $Mg_{0.13}$ = 0.81 from chemical analysis, to be compared with 0.82 Al a.p.f.u., from the refinement), with a minor contribution of heavier scatterers ($Fe^{3+}_{0.14}Mn^{3+}_{0.12}$ = 0.26 a.p.f.u. *vs.* 0.18 Fe a.p.f.u. from the refinement, Table 4). The observed average bond length at *M* sites (1.962 Å, Table 6) is too short for Fe^{2+} and Mn^{2+}. In addition, incident bond valence at the *M* site is in agreement with average charge being dominantly 3+, i.e. considering both Fe^{3+} and Mn^{3+} at the *M* sites. The trivalent oxidation state of Fe and Mn agrees with the oxidized nature of the ore. Therefore, both elements were considered to be in a trivalent oxidation state for formula calculation (see chemistry above). Site distribution at the *A* sites was obtained according to the structure refinement that shows a clear difference in scattering in both sites: 29.9(1) electrons per site at the *A*(1) site and 39.4(2) electrons per site at the *A*(2) site. Therefore, $Sr_{0.55}Ca_{0.45}$ is assigned to *A*(1) and $Sr_{0.92}Ba_{0.08}$ to *A*(2). Bond-valence calculations indicate that both the *A*(1) and *A*(2) sites are compatible with the dominance of divalent cations at these sites. Site-scattering values obtained for *T* sites are equal, although average bond lengths and distortion parameters were significantly different (Table 6). The limited quantity of V observed in WDS analyses and the absence of high-charge cations that may potentially enter the *T* sites (P, S, Si) lead to V being considered disordered equally among both sites. The distortion is therefore interpreted as an intrinsic feature of the structure. The cation sums at *T* sites implies $T_4^{5+}M_2^{3+}A_4^{2+}$ which accounts for 34^+.

TABLE 3. Crystal data and summary of parameters describing the data collection and refinement for grandaite.

Crystal system	Monoclinic
Space group	$P2_1/m$
Unit-cell dimensions	
a (Å)	7.5764(5)
b (Å)	5.9507(4)
c (Å)	8.8050(6)
β (º)	112.551(2)
V (Å^3)	366.62(4)
Z	2
μ (mm^{-1})	20.34
F(000)	443
D_{calc} (g cm^{-3})	4.378
Crystal size (mm)	0.130 × 0.085 × 0.080
Radiation type	Mo$K\alpha$ (0.71073 Å)
Temperature (K)	298
θ range for data collection (º)	2.5–35.0
R_{int}	0.026
Reflections collected	6095
Independent reflections	1734
F_o>4σ(F)	1442
Refinement method	least-squares matrix: full
No. of refined parameters	84
Final R_{obs}	0.037
R_1	0.029
wR_2 F_o>4σ(F)	0.065
Highest peak/deepest hole (e Å^{-3})	+2.57 / −0.76
Goodness of fit on F^2	1.074

TABLE 4. Multiplicities, fractional atom coordinates and equivalent isotropic displacement parameters (Å^2) for grandaite*.

Site	Mult.	Occ.	x/a	y/b	z/c	U_{iso}
T(1)	2e	0.886(9)As 0.114(9)V	0.43733(5)	¼	0.17111(4)	0.0124(1)
T(2)	2e	0.884(9)As 0.116(9)V	0.03113(4)	¼	0.33393(4)	0.0103(1)
M	2a	0.815(5)Al 0.185(5)Fe	0	0	0	0.0106(2)
A(1)	2e	0.548(5)Sr 0.452(5)Ca	0.25931(6)	¼	0.73723(5)	0.0188(1)
A(2)	2e	0.921(7)Sr 0.079(7)Ba	0.67546(4)	¼	0.58860(4)	0.0133(1)
O(1)	4f		0.0231(3)	0.5144(3)	0.7853(2)	0.0203(4)
O(2)	2e		0.2635(4)	¼	0.4501(3)	0.0265(6)
O(3)	2e		0.9109(4)	¼	0.4550(4)	0.0320(7)
O(4)	4f		0.5055(2)	0.0223(3)	0.2905(2)	0.0197(4)
O(5)	2e		0.5209(5)	¼	0.0207(4)	0.0391(8)
O(6)	2e		0.1923(3)	¼	0.0638(3)	0.0210(5)
O(7)	2e		0.8303(3)	¼	0.9207(3)	0.0137(5)
H(7)	2e	1.000	0.7043	¼	0.9230	0.0200

* The temperature factor has the form exp($-T$) where $T = 8\pi^2 U(\sin(\theta)/\lambda)^2$ for isotropic atoms.

TABLE 5. Anisotropic displacement parameters (Å^2) for grandaite*.

Site	U^{11}	U^{22}	U^{33}	U^{23}	U^{13}	U^{12}
T(1)	0.0124(2)	0.0114(2)	0.0114(2)	0	0.00242(12)	0
T(2)	0.0124(2)	0.0105(2)	0.0093(2)	0	0.00556(12)	0
M	0.0139(4)	0.0087(4)	0.0090(4)	0.0000(2)	0.0039(3)	−0.0004(2)
A(1)	0.0179(2)	0.0206(2)	0.0226(2)	0	0.0131(2)	0
A(2)	0.0147(2)	0.01477(14)	0.01246(15)	0	0.00758(10)	0
O(1)	0.0330(1)	0.0132(7)	0.0156(8)	0.0020(6)	0.0105(7)	0.0025(6)
O(2)	0.0152(12)	0.040(2)	0.0217(13)	0	0.0041(10)	0
O(3)	0.0334(15)	0.041(2)	0.035(2)	0	0.0273(14)	0
O(4)	0.0226(8)	0.0153(8)	0.0177(8)	0.0026(6)	0.0039(7)	0.0017(6)
O(5)	0.041(2)	0.059(2)	0.028(2)	0	0.0249(14)	0
O(6)	0.0149(11)	0.0216(12)	0.0207(12)	0	0.0005(9)	0
O(7)	0.0121(10)	0.0150(11)	0.0124(10)	0	0.0029(8)	0

* The temperature factor has the form $\exp(-T)$ where $T = 2\pi^2\Sigma_{ij}(h(i)h(j)U(i,j)a^*(i)a^*(j)$.

Anion sites

There are seven anion positions in the structure of grandaite, two of them on general positions, accounting for a total of 18 anions per unit cell. The bond-valence table (Table 7) shows that one of seven anion sites shows a bond-valence incidence close to 2 vu (valence units), while the *O*(7) site has a lower contribution (1.272 vu) compatible with a monovalent anion at this site. The absence of F in the chemical analyses (Table 2) indicates that this site must therefore host a hydroxyl group. In fact, a maximum was

TABLE 6. Selected interatomic distances (Å) and angles (°) for grandaite*.

T(1) −*O*(4) (×2)	1.671(2)	*A*(1) −*O*(4)(×2)	2.489(2)
−*O*(5)	1.673(3)	−*O*(5)	2.523(3)
−*O*(6)	1.730(2)	−*O*(1) (×2)	2.537(2)
<*T*(1)−*O*>	1.686	−*O*(2)	2.541(3)
V (Å^3)	2.449	−*O*(3)	2.848(3)
σ^2*	12.93	−*O*(6)	3.105(3)
λ*	1.0034	<*A*(1)−*O*>	2.634
		V (Å^3)	26.80
T(2) −*O*(3)	1.647(3)		
−*O*(2)	1.663(3)	*A*(2)−*O*(3)	2.485(3)
−*O*(1) (×2)	1.704(2)	−*O*(4) (×2)	2.600(2)
<*T*(2)−*O*>	1.680	−*O*(7)	2.701(3)
V (Å^3)	2.430	−*O*(4) (×2)	2.791(2)
σ^2*	0.49	−*O*(2)	2.883(3)
λ*	1.0006	−*O*(1) (×2)	2.986(2)
		−*O*2 (×2)	3.050(1)
M −*O*(7) (×2)	1.914(1)	<*A*(2)−*O*>	2.811
−*O*(1) (×2)	1.966(2)	*V* (Å^3)	49.28
−*O*(6) (×2)	2.006(2)		
<*M* −*O*>	1.962	*O*(7)–*H*(7)	0.96
V (Å^3)	9.934	*O*(7)···*O*(5)	2.80
σ^2*	32.00	*O*(5)···*H*(7)	1.89
λ*	1.0097		

* Mean quadratic elongation (λ) and the angle variance (σ^2) were calculated according to Robinson *et al.* (1971).

TABLE 7. Bond-valence calculations for grandaite.

Site	*T*(1)	*T*(2)	*M*	*A*(1)	*A*(2)	*H*(7)	Σ
O(1)		$1.17^{\times 2\downarrow}$	$0.46^{\times 2\downarrow}$	$0.27^{\times 2\downarrow}$	$0.10^{\times 2\downarrow}$		2.00
O(2)		1.30		0.27	0.13 $0.09^{\times 2\downarrow}$ $_{\times 2\rightarrow}$		1.88
O(3)		1.35		0.11	0.37		1.83
O(4)	$1.27^{\times 2\downarrow}$			$0.30^{\times 2\downarrow}$	$0.27^{\times 2\downarrow}$ $0.17^{\times 2\downarrow}$		2.01
O(5)	1.27			0.28		0.18	1.73
O(6)	1.10		$0.42^{\times 2\downarrow}$ $_{\times 2\rightarrow}$	0.07			2.01
O(7)			$0.53^{\times 2\downarrow}$ $_{\times 2\rightarrow}$		0.21	0.81	2.08
b.v.	4.91	4.99	2.82	1.87	1.97	0.99	17.55
Agg. ch.	5.00	5.00	2.88	2.00	1.98	1.00	17.86

b.v. = bond valence; Agg. ch. = aggregate charge.

found at ~0.96 Å in the Fourier difference and added to the model as atom H(7). The H at *H*(7) is at 1.895 Å from the O(5) atom which has a bond-valence sum of 1.55 vu and so is likely to receive a H bond. Therefore, there is a H bond with O at *O*(5) ensuring a further contribution of bond valence to this site (Table 7). The structural model thus confirms O−H···O = 2.8 Å, in good agreement with IR data. The anion part of the structure is $O_{16}(OH)_2$, which accounts for 34^-.

Structure topology

The crystal structure of grandaite (Figs 5−6) is topologically identical to that of arsenbrackebuschite. Chains of $[M^{3+,2+}(T^{5+}O_4)_2(OH, H_2O)]$ units are connected through interstitial divalent cations. The M^{3+} octahedron shares edges with other octahedra forming a chain along [010]. The shared edge has one anion that can be an OH group or a H_2O molecule, depending on the charge of the cation at the octahedron and the other anion is shared with the apex of a $T^{5+}O_4$ tetrahedron (the *T*(1) site). The remaining four anions coordinating the octahedron are linked to the edge of another $T^{5+}O_4$ tetrahedron (the *T*(2) site) alternating in both sides (Fig. 6). Minor V is disordered among the two arsenate tetrahedra. Decorated chains of octahedra link together through bonding with two symmetrically independent interstitial cations at the *A*(1) and *A*(2) sites and H bonding (O···O = 2.8 Å). Minor Ca orders preferentially in the smaller eight-coordinated *A*(1) site (<*A*(1)−O> = 2.634 Å), while minor Ba orders in the larger 11-coordinated *A*(2) site (<*A*(2)−O> = 2.811 Å) in grandaite. In arsenbrackebuschite Pb occupies both sites but is shifted off-centre as is usual for its lone-pair configuration. The small quantity of Pb found in grandaite at the *A*(2′) site also follows this configuration. This Pb off-centre displacement has been reported previously e.g.: synthetic $Pb_2(Pb,K)_4[Si_8O_{20}]O$ (Moore *et al*., 1985); Pb replacing Ba in hyalotekite (Moore *et al*., 1982; Christy *et al*., 1998); or Pb replacing *REE* in lusernaite-(Y) (Biagioni *et al*., 2013). The distortion observed for the *T*(2) site, along with the low bond-valence incidence at *O*(5) represents a stressed environment for this structure.

Related minerals

Grandaite, $Sr_2Al(AsO_4)_2(OH)$, is the As-dominant analogue of goedkenite, $Sr_2Al(PO_4)_2(OH)$ and the Sr-As-dominant analogue of bearthite, $Ca_2Al(PO_4)_2(OH)$. It is the first Al member of the arsenbrackebuschite group in the brackebuschite supergroup (Table 8). The brackebuschite supergroup has the general formula $^{viii,xi}A_2^{2+,1+}\ ^{vi}M^{3+,2+}\ H_{0-1}[^{iv}(T^{5+,6+})O_4]_2[O_y,(OH)_{1-y}]$. Subgroups are divided on the basis of the charge species dominance at the *T* sites. The crystal chemistry of this supergroup is under study as part of a broader project. A comparison of the properties of the members of the arsenbrackebuschite group is reported in Table 9. In the Strunz System (Strunz and Nickel, 2001) grandaite fits in subdivision 8.B.G, phosphates, etc. with

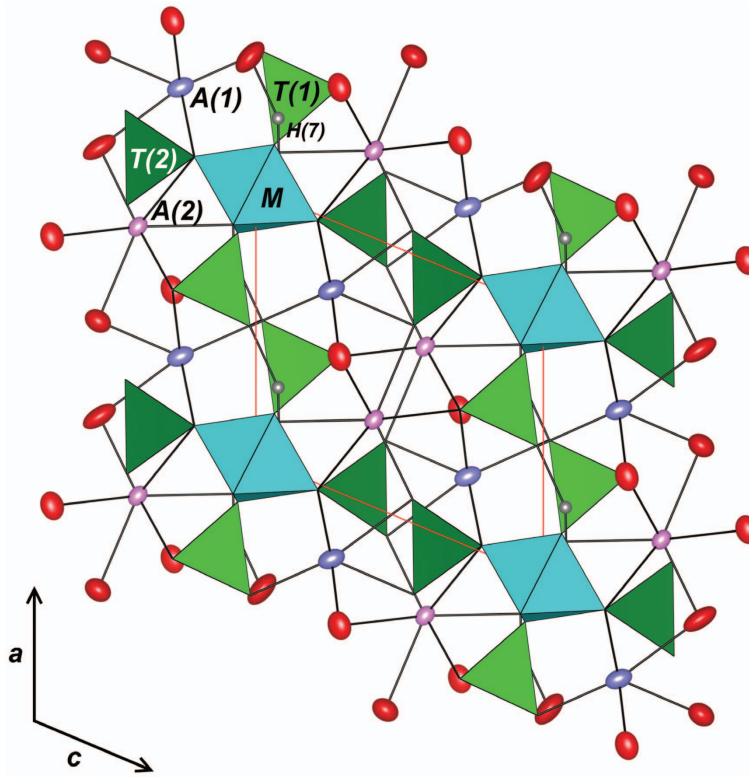

FIG. 5. Projection of the grandaite structure down [010]; the unit cell is indicated by thick red lines. Ellipsoids at 90% probability. Atom sites labelled in the figure are: *T*(1): light green, *T*(2): dark green, *M*: light blue, *A*(1): lilac, *A*(2): violet, *H*(7): grey, oxygen sites: red. Drawing obtained with *VESTA 3* (Momma and Izumi, 2011).

additional anions, without H_2O, with medium-sized and large cations, (OH, etc.).

Isotypic structures occur in the synthetic compounds $Na_2Cr^{3+}(Cr^{6+}O_4)_2(OH)$, $K_2Cr^{3+}(Cr^{6+}O_4)_2(OH)$ (Jonsson, 1970) and $Pb_3(P_{1.15}V_{0.85})_2O_8$ (Kiat *et al.*, 1993). The minerals fornacite, $Pb_2Cu^{2+}[(CrO_4)(AsO_4)](OH)$ (Lacroix, 1915, 1916; Cocco *et al.*, 1967; Fanfani

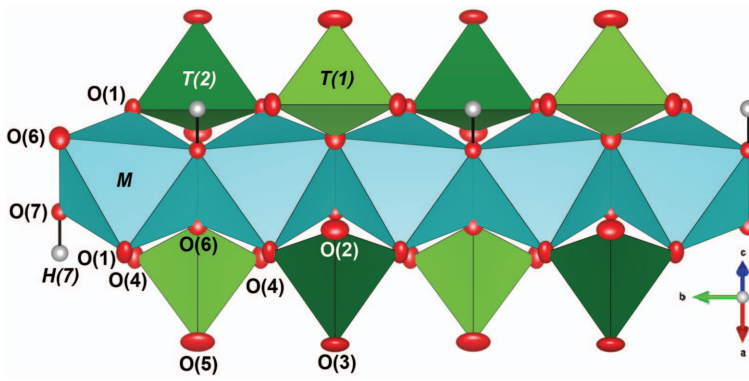

FIG. 6. Detail of the chain of *M* octahedra. Ellipsoids at 50% probability. Atom sites labelled in the figure; colours as in Fig. 5. Drawing obtained with *VESTA 3* (Momma and Izumi, 2011).

TABLE 8. Minerals of the brackebuschite supergroup. References are given in brackets.

Brackebuschite supergroup, $A(1)^{2+}\ A(2)^{2+}\ {}^{vi}[M_x^{3+},M_{1-x}^{2+}]\ [{}^{iv}(T_z^{5+},T_{1-z}^{6+})O_4]_2\ (O_{1-y}OH_y)$			
Arsenbrackebuschite group As dominant at T	Brackebuschite group V dominant at T	Goedkenite group P dominant at T	Tsumebite group P or As + S or V dominant at T
Arsenbrackebuschite [1,2] $Pb_2Fe^{3+}(AsO_4)_2(OH,H_2O)$	Brackebuschite [7,8,9,10] $Pb_2Mn^{3+}(VO_4)_2(OH)$	Bearthite [17,18,19] $Ca_2Al(PO_4)_2(OH)$	Arsentsumebite [3,4,5,29] $Pb_2Cu[(AsO_4)(SO_4)](OH)$
Feinglosite [6] $Pb_2Zn(AsO_4)_2(OH,H_2O)$	Calderónite* [11] $Pb_2Fe^{3+}(VO_4)_2(OH)$	Goedkenite [23] $Sr_2Al(PO_4)_2(OH)$	Bushmakinite [20,21,22] $Pb_2Al[(PO_4)(VO_4)](OH)$
Grandaite [30] $Sr_2Al(AsO_4)_2(OH)$	Gamagarite [12,13,14] $Ba_2Fe^{3+}(VO_4)_2(OH,H_2O)$		Tsumebite [9,24,25,26,27,28,29] $Pb_2Cu[(PO_4)(SO_4)](OH)$
	Heyite* [15] $Pb_5Fe_2^{2+}(VO_4)_2O_4$		
	Tokyoite [16] $Ba_2Mn^{3+}(VO_4)_2(OH)$		

Refs: [1] Abraham *et al.* (1978); [2] Hofmeister and Tillmanns (1978); [3] Vésignié (1935); [4] Bideaux *et al.* (1966); [5] Zubkova *et al.* (2002); [6] Clark *et al.* (1997); [7] Rammelsberg (1880); [8] Donaldson and Barnes (1955); [9] Fanfani and Zanazzi (1967); [10] Foley *et al.* (1997); [11] González del Tánago *et al.* (2003); [12] de Villiers (1943); [13] Harlow *et al.* (1984); [14] Basso *et al.* (1987); [15] Williams (1973); [16] Matsubara *et al.* (2004); [17] Chopin *et al.* (1993); [18] Brunet and Chopin (1995); [19] Roth (2007); [20] Pekov *et al.* (2002); [21] Yakubovich *et al.* (2002); [22] Pekov (2007); [23] Moore *et al.* (1975); [24] Rosický (1912); [25] Busz (1912); [26] Spencer (1913); [27] LaForge (1938); [28] Nichols (1966); [29] Schlüter *et al.* (1994); [30] this study. *Needs further study.

and Zanazzi, 1968) and vauquelinite, $Pb_2Cu^{2+}[(CrO_4)(PO_4)](OH)$ (Berzelius, 1818; Fanfani and Zanazzi, 1968), the members of the törnebohmite group [törnebohmite-(Ce), $Ce_2Al(SiO_4)_2(OH)$ and törnebohmite-(La), $La_2Al(SiO_4)_2(OH)$ (Geijer, 1921; Wherry, 1921; Shen and Moore, 1982)], molybdofornacite, $Pb_2Cu^{2+}[(MoO_4)(AsO_4)](OH)$ (Medenbach *et al*., 1983) and the potential, but never approved, P-analogue of molybdofornacite, $Pb_2Cu^{2+}[(MoO_4)(PO_4)](OH)$, (Nickel and Hitchen, 1994) present derivative structure analogues characterized by doubling of one unit-cell parameter or a shift in the origin (and different symmetry). These structures are topologically identical to brackebuschite supergroup structures, the doubling of the cell being due to ordering of anions in the structure of fornacite and

TABLE 9. Comparison of minerals of the arsenbrackebuschite group.

	Arsenbrackebuschite	Feinglosite*	Grandaite
Reference	(1,2)	(3)	This work
Formula	$Pb_2Fe^{3+}(AsO_4)_2(OH,H_2O)$	$Pb_2Zn(AsO_4)_2{\cdot}H_2O$	$Sr_2Al(AsO_4)_2(OH)$
System	Monoclinic	Monoclinic	Monoclinic
Space group	$P2_1/m$	$P2_1$, $P2_1/m$	$P2_1/m$
a (Å)	7.764(2)	7.766(6)	7.5764(5)
b	6.045(2)	5.955(3)	5.9507(4)
c	9.022(2)	8.973(6)	8.8050(5)
β (º)	112.5	112.20(6)	112.551(1)
V (Å^3)	391.2	384.2(4)	366.62(4)
Z	2	2	2
a:b:c	1.2843:1:1.4924	1.5068: 1:1.3041	1.273:1:1.480
D_{meas} (g cm^{-3})	n.d.	n.d.	n.d.
D_{calc} (g cm^{-3})	6.54	6.52	4.38
Strongest lines in the powder pattern: d_{obs} (Å)(I)	3.012 (100), 3.268 (90), 2.777 (60), 2.313 (30), 2.133 (30), 4.92 (25), 3.68 (25)	3.246(100), 2.988(60), 2.769 (60), 4.85(50), 2.107(50), 3.659 (30), 2.293 (30)	3.194 (100), 2.705 (65), 2.087 (52), 2.981 (51), 2.922 (40), 2.743 (31), 1.663 (28), 1.685 (25)
Optical (sign)	biaxial (−)	n.d.	biaxial (+)
α	n.d.	n.d.	1.726(1)
β	n.d.	n.d.	1.731(1)
γ	n.d.	n.d.	1.752(1)
2V(º)	n.d.	n.d.	52(2) (meas), 53 (calc)
Colour	honey-yellow, yellow, brown, green	pale olive-green	orange to salmon to brown
Pleochroism	honey-yellow to bright yellow	non pleochroic	non-pleochroic
Hardness (Mohs)	4−5	4−5	6−6.5
Streak	pale brownish	white	reddish brown
Lustre	resinous to adamantine	adamantine	vitreous
Fluorescent	−	−	non-fluorescent
Tenacity	−	sectile	brittle
Cleavage	perfect on {010}	−	not observed
Twinning	complex, observed	−	none observed
Habit and forms	tiny flat plates and laths	multiple individuals, in radiating botryoidal aggregates subhedral grains	
Association	beudantite, anglesite, mimetite, bayldonite, stolzite	goethite, anglesite, wulfenite, chalcocite, arsendescloizite, gypsum	aegirine, adelite, baryte, braunite, hematite, quartz, tilasite, unidentified Mn oxides and Mn silicates

Refs: [(1)]Abraham *et al*. (1978); [(2)]Hofmeister and Tillmanns (1978); [(3)]Clark *et al*. (1997).
* unit-cell parameters transformed to compare the structure relationships between group phases.

the shift of the origin and different symmetry elements due to order of Cu at the *M* sites in vauquelinite, probably due to Jahn-Teller effects. The latter are also structurally related to the members of descloizite, fairfieldite, roselite and tsumcorite groups.

Acknowledgements

The authors thank Bruno Lombardo (CNR-IGG-Torino) for his assessment support in field work at the Valletta and Fabio Bellatreccia (Università di Roma Tre) for providing IR data. FC acknowledges Chiara Domeneghetti (Università di Pavia) for access to the Bruker AXS diffractometer under a collaboration agreement between the Dipartimento di Scienze della Terra (Università di Torino) and the Dipartimento di Scienze della Terra e Ambiente (Università di Pavia). Carmelo Sibio (Università di Torino) is thanked for thin-section preparation. Raul Carampin (CNR-IGG-Padova, Italy) is thanked for support with the WDS analysis. Cristian Biagioni, Mark Welch and Pete Leverett are thanked for their constructive reviews. FC, PB and EC acknowledge the support of the project "PROactive Management of GEOlogical Heritage in the PIEMONTE Region" (www.progeopiemonte.it/en) co-founded by the University of Turin – Compagnia di San Paolo Bank Foundation "JCAPC - Progetti di Ateneo 2011" grant on line B1 "Experimental Sciences and Technology" (Project Id: ORTO11Y7HR, P.I. Prof. Marco Giardino). FC and EB thank the MIUR and the AMI for the co-funding of a research contract for EB for the year 2013.

References

Abraham, K., Kautz, K., Tillmanns, E. and Walenta, K. (1978) Arsenbrackebuschite, $Pb_2(Fe,Zn)(OH,H_2O)[AsO_4]_2$, a new arsenate mineral. *Neues Jahrbuch für Mineralogie*, *Monatshefte*, **1978**, 193–196.

Antofilli, M., Borgo, E. and Palenzona, A. (1983) *I nostri minerali. Geologia e mineralogia in Liguria*. SAGEP Editrice, Genoa, Italy, 296 pp. [in Italian].

Basso, R., Palenzona, A. and Zefiro, L. (1987) Gamagarite: new occurrence and crystal structure refinement. *Neues Jahrbuch für Mineralogie, Monatshefte*, **1987**, 295–304.

Biagioni, C., Bonaccorsi, E., Cámara, F., Cadoni, M., Ciriotti, M.E., Bersani, D. and Kolitsch, U. (2013) Lusernaite-(Y), $Y_4Al(CO_3)_2(OH,F)_{11}\cdot 6H_2O$, a new mineral species from Luserna Valley, Piedmont, Italy: Description and crystal structure. *American Mineralogist*, **98**, 1322–1329.

Berzelius, J. (1818) Undersökning af ett hittills obemärkt Fossil, som stundom följer den Siberiska kromsyrade blyoxiden. *Afhandlingar i Fysik, Kemi och Mineralogi*, **6**, 246–254 [in Swedish].

Bideaux, R.A., Nichols, M.C. and Williams, S.A. (1966) The arsenate analog of tsumebite, a new mineral. *American Mineralogist*, **51**, 258–259.

Borgo, E. and Palenzona, A. (1988) *I nostri minerali. Geologia e mineralogia in Liguria. Aggiornamento* 1988. SAGEP Editrice, Genoa, Italy, 48 pp. [in Italian].

Brown, I.D. (1981) The bond-valence method: an empirical approach to chemical structure and bonding. Pp. 1–30 in: *Structure and Bonding in Crystals* II (M. O'Keeffe and A. Navrotsky, editors). Academic Press, New York.

Brugger, J. and Gieré, R. (1999) As, Sb, and Ce enrichment in minerals from a metamorphosed Fe-Mn deposit (Val Ferrera, Eastern Swiss Alps). *The Canadian Mineralogist*, **37**, 37–52.

Bruker AXS (2003) *SAINT*. Data Reduction Software, version 6.45A. Wisconsin, USA.

Brunet, F. and Chopin, C. (1995) Bearthite, $Ca_2Al(PO_4)_2OH$: stability, thermodynamic properties and phase relations. *Contributions to Mineralogy and Petrology*, **121**, 258–266.

Busz, K. (1912) Tsumebit, ein neues Mineral von Otavi und Zinnsteinkristalle. *Deutschen Naturforscher und Artze in Münster*, **84**, 230–230 [in German].

Chopin, C., Brunet, F., Gebert, W., Medenbach, O. and Tillmanns, E. (1993) Bearthite, $Ca_2Al[PO_4]_2(OH)$, a new mineral from high-pressure terranes of the western Alps. *Schweizerische Mineralogische und Petrographische Mitteilungen*, **73**, 1–9.

Christy, A.G., Grew, E.S., Mayo, S.C., Yates, M.G. and Belakovskiy, D.I. (1998) Hyalotekite, $(Ba,Pb,K)_4(Ca,Y)_2Si_8(B,Be)_2(Si,B)_2O_{28}F$, a tectosilicate related to scapolite: new structure refinement, phase transitions and a short-range ordered 3b superstructure. *Mineralogical Magazine*, **62**, 77–92.

Clark, A.M., Criddle, A.J., Roberts, A.C., Bonardi, M. and Moffatt, E.A. (1997) Feinglosite, a new mineral related to brackebuschite, from Tsumeb, Namibia. *Mineralogical Magazine*, **61**, 285–289.

Cocco, G., Fanfani, L. and Zanazzi, P.F. (1967) The crystal structure of fornacite. *Zeitschrift für Kristallographie*, **124**, 385–397.

de Villiers, J.E. (1943) Gamagarite, a new vanadium mineral from the Postmasburg manganese deposits. *American Mineralogist*, **28**, 329–335.

Donaldson, D.M. and Barnes, W.H. (1955) The structures of the minerals of the descloizite group and adelite groups: III – brackebuschite. *American Mineralogist*, **40**, 597–613.

Emsley, J. (2011) Arsenic. Pp. 47–55 in: *Nature's Building Blocks: An A–Z Guide to the Elements*. Oxford University Press, Oxford, UK.

Fanfani, L. and Zanazzi, P.F. (1967) Structural similarities of some secondary lead minerals. *Mineralogical Magazine*, **36**, 522–529.

Fanfani, L. and Zanazzi, P.F. (1968) The crystal structure of vauquelinite and the relationships to fornacite. *Zeitschrift für Kristallographie*, **126**, 433–443.

Foley, J.A., Hughes, J.M. and Lange, D. (1997) The atomic arrangement of brackebuschite, redefined as $Pb_2(Mn^{3+},Fe^{3+})(VO_4)_2(OH)$, and comments on Mn^{3+} octahedra. *The Canadian Mineralogist*, **35**, 1027–1033.

Franchi, S. and Stella, A. (1930*) Carta Geologica d'Italia 1:100.000: Foglio 78–79* (Argentera-Dronero). 1[a] edizione. Regio Ufficio Geologico. Stabilimento Tipografico L. Salomone, Rome [in Italian].

Frost, R.L. and Keeffe, E.C. (2011) The mixed anion mineral parnauite $Cu_9[(OH)_{10}|SO_4|(AsO_4)_2]\cdot 7H_2O$ – A Raman spectroscopic study. *Spectrochimica Acta Part A*, **81**, 111–116.

Geijer, P. (1921) The cerium minerals of Bastnäs at Riddarhyttan. *Sveriges Geologiska Undersökning Årsbok*, **C304**, 3–24.

Gidon, M., Kerchove, C., Michard, A., Tricart, P. and Goffé, B. (1994) *Carte Géologique de la France à 1:50.000. Feuille Aiguille de Chambeyron (872)*. Notice Explicative. BRGM, Service Géologique National, Orléans, France [in French].

González del Tánago, J., La Iglesia, Á., Rius, J. and Fernández Santín, S. (2003) Calderónite, a new lead-iron-vanadate of the brackebuschite group. *American Mineralogist*, **88**, 1703–1708.

Hak, J., Johan, Z., Kvaček, M. and Liebscher, W. (1969) Kemmlitzite, a new mineral of the woodhouseite group. *Neues Jahrbuch für Mineralogie, Monatshefte*, **1969**, 201–212.

Harlow, G.E., Dunn, P.J. and Rossman, G.R. (1984) Gamagarite: a re-examination and comparison with brackebuschite-like minerals. *American Mineralogist*, **69**, 803–806.

Hofmeister, W. and Tillmanns, E. (1978) Strukturelle untersuchungen an arsenbrackebuschit. *Tschermaks Mineralogische und Petrographische Mitteilungen*, **25**, 153–163 [in German].

Horiba Jobin Yvon (2004, 2005) *LabSpec software for Raman spectroscopic data analysis, acquisition and manipulation. Version 5.64.15*. HORIBA Jobin Yvon SAS, Villeneuve d'Ascq, France.

Jonsson, O. (1970) The crystal structure of $Na_2Cr_3O_8OH$ and $K_2Cr_3O_8OH$. *Acta Chemica Scandinavica*, **24**, 3627–3644.

Kiat, J.M., Garnier, P., Calvarin, G. and Pinot, M. (1993) Structural study of lead orthophosphovanadates: role of the electron lone pairs in the phase transitions. *Journal of Solid State Chemistry*, **103**, 490–503.

Lacroix, A. (1915) Note préliminaire sur une nouvelle espèce minérale (furnacite), provenant du Moyen Congo (Afrique équatoriale française). *Bulletin de la Société française de Minéralogie*, **38**, 198–200 [in French].

Lacroix, A. (1916) Erratum concernant une nouvelle espèce minérale du Congo. *Bulletin de la Société française de Minéralogie*, **39**, 84–84 [in French].

LaForge, L. (1938) Crystallography of tsumebite. *American Mineralogist*, **23**, 772–782.

Larson, A.C. and Von Dreele, R.B. (1994) *General Structure Analysis System (GSAS)*. Los Alamos National Laboratory Report LAUR, 86–748. Los Alamos National Laboratory, New Mexico.

Lefèvre, R. (1982) *Les nappes briançonnaises internes et ultra-briançonnaises dans les Alpes Cottiennes méridionales*. Thèse Scientifique, Université Paris Sud - Paris XI, Orsay, France [in French].

Libowitzky, E. (1999) Correlation of O–H stretching frequencies and O–H···O hydrogen bond lengths in minerals. *Monatshefte für Chemie*, **130**, 1047–1059.

Mandarino, J.A. (1979) The Gladstone-Dale relationship. Part III. Some general applications. *The Canadian Mineralogist*, **17**, 71–76.

Mandarino, J.A. (1981) The Gladstone-Dale retationship. Part IV. The compatibility concept and its application. *The Canadian Mineralogist*, **19**, 441–450.

Mangione, T.G. (1999) Allume, vetriolo, ferro: attività minerarie e metallurgiche nel marchesato di Saluzzo (secoli XIV–XVI). Pp. 79–101 in: *Miniere, fucine, metallurgia nel Piemonte medievale e moderno* (R. Comba, editor). Società per gli Studi Storici Archeologici e Artistici della Provincia di Cuneo, Centro studi storico-etnografici, Museo provinciale "Augusto Doro", Rocca de' Baldi, Cuneo, Italy [in Italian].

Matsubara, S., Miyawaki, R., Yokoyama, K., Shimizu, M. and Imai, H. (2004) Tokyoite, $Ba_2Mn^{3+}(VO_4)_2(OH)$, a new mineral from the Shiromaru mine, Okutama, Tokyo, Japan. *Journal of Mineralogical and Petrological Sciences*, **99**, 363–367.

Medenbach, O., Abraham, K. and Gebert, W. (1983) Molybdofornacit, ein neues Blei–Kupfer–Arsenat–Molybdat–Hydroxid von Tsumeb, Namibia. *Neues Jahrbuch für Mineralogie, Monatshefte*, **1983**, 289–295 [in German].

Momma, K. and Izumi, F. (2011) *VESTA 3* for three-dimensional visualization of crystal, volumetric and morphology data. *Journal of Applied Crystallography*, **44**, 1272–1276.

Moore, P.B., Irving, A.J. and Kampf, A.R. (1975)

Foggite, $CaAl(OH)_2(H_2O)[PO_4]$; goedkenite, $(Sr,Ca)_2Al(OH)[PO_4]_2$; and samuelsonite $(Ca,Ba)Fe_2^{2+}Mn_2^{2+}Ca_8Al_2(OH)_2[PO_4]_{10}$: three new species from the Palermo No. 1 Pegmatite, North Groton, New Hampshire. *American Mineralogist*, **60**, 957–964.

Moore, P.B., Araki, T. and Ghose, S. (1982) Hyalotekite, a complex lead borosilicate: Its crystal structure and the lone-pair effect of Pb(II). *American Mineralogist*, **67**, 1012–1020.

Moore, P.B., Sen Gupta, P.K. and Schlemper, E.O. (1985) Solid solution in plumbous potassium oxysilicate affected by interaction of a lone pair with bond pairs. *Nature*, **318**, 548–550.

Mukherjee, A., Sengupta, M.K. and Hossain, M.A. (2006) Arsenic contamination in groundwater: A global perspective with emphasis on the Asian scenario. *Journal of Health Population and Nutrition*, **24**, 142–163.

Myneni, S.C.B., Traina, S.J., Waychunas, G.A. and Logan, T.J. (1998*a*) Experimental and theoretical vibrational spectroscopic evaluation of arsenate coordination in aqueous solutions and solids. *Geochimica et Cosmochimica Acta*, **62**, 3285–3300.

Myneni, S.C.B., Traina, S.J., Waychunas, G.A. and Logan, T.J. (1998*b*) Vibrational spectroscopy of functional group chemistry and arsenate coordination in ettringite. *Geochimica et Cosmochimica Acta*, **62**, 3499–3514.

Nakamoto, K. (1986) *Infrared and Raman Spectra of Inorganic and Coordination Compounds*. Wiley, New York.

Nichols, M.C. (1966) The structure of tsumebite. *American Mineralogist*, **51**, 267–267.

Nickel, E.H. and Hitchen, G. (1994) The phosphate analog of molybdofornacite from Whim Creek, Western Australia. *Mineralogical Record*, **25**, 203–204.

Norman, N.C. (editor) (1998) *Chemistry of arsenic, antimony and bismuth*. Blackie Academic and Professional, London, 483 pp.

Palenzona, A. (1991) *I nostri minerali. Geologia e mineralogia in Liguria. Aggiornamento 1990*. Amici Mineralogisti Fiorentini, Associazione Piemontese Mineralogia Paleontologia & Mostra Torinese Minerali, Centro Mineralogico Varesino, Gruppo Mineralogico "A. Negro" Coop Liguria (GE), Gruppo Mineralogico Lombardo, Gruppo Mineralogico Paleontologico "3M", SAGEP, Genoa, Italy [in Italian].

Palenzona, A. (1996) I nostri minerali. Geologia e mineralogia in Liguria, Aggiornamento 1995. *Rivista Mineralogica Italiana*, **2**, 149–172 [in Italian].

Pekov, I.V. (2007) New minerals from former Soviet Union countries, 1998–2006: new minerals approved by the IMA Commission on New Minerals and Mineral Names. *Mineralogical Almanac*, **11**, 9–51.

Pekov, I.V., Kleimenov, D.A., Chukanov, N.V., Yakubovich, O.V., Massa, W., Belakovskiy, D.I. and Pautov, L.A. (2002) Bushmakinite $Pb_2Al(PO_4)(VO_4)(OH)$, a new mineral of the brackebuschite group from oxidized zone of Berezovskoye gold deposit, the Middle Urals. *Zapiski Vserossijskogo Mineralogicheskogo Obshchestva*, **131**, 62–71.

Piccoli, G.C. (editor) (2002) Minerali delle Alpi Marittime e Cozie Provincia di Cuneo. Pp. 147–148 in: *Amici del Museo* "F. Eusebio". Alba, Cuneo, Italy [in Italian].

Pipino, G. (2010) *Documenti minerari degli stati sabaudi*. Museo Storico dell'Oro Italiano, Tipografia Pesce, Ovada (Alessandria), Italy, 323 pp. [in Italian].

Pouchou, J.L. and Pichoir, F. (1984) A new model for quantitative analysis: Part I. Application to the analysis of homogeneous samples. *La Recherche Aerospatiale*, **3**, 13–38.

Pouchou, J.L. and Pichoir, F. (1985) '*PAP*' $\varphi(\rho Z)$ procedure for improved quantitative microanalysis. Pp. 104–106 in: *Microbeam Analysis* (J.T. Armstrong, editor). San Francisco Press, San Francisco, California, USA.

Rammelsberg, C. (1880) Über die vanadinerze aus dem Staat Córdoba in Argentinien. *Zeitschrift der Deutschen Geologischen Gesellschaft*, **32**, 708–713 [in German].

Robinson, K., Gibbs, G.V. and Ribbe, P.H. (1971) Quadratic elongation: a quantitative measure of distortion in coordination polyhedra. *Science*, **172**, 567–570.

Rosický, V. (1912) Preslit, ein neues Mineral von Tsumeb in Deutsch-Südwestafrika. *Zeitschrift für Krystallographie und Mineralogie*, **51**, 521–526 [in German].

Roth, P. (2007) Bearthite. Pp. 44–45 in: *Minerals first discovered in Switzerland and minerals named after Swiss individuals*. Kristallografik Verlag, Achberg, Germany.

Schlüter, J., Gebhard, G. and Wappler, G. (1994) Tsumebit oder Arsentsumebit aus Tsumeb? *Lapis*, **19(10)**, 31–34 [in German].

Sheldrick, G.M. (2008) A short history of *SHELX*. *Acta Crystallographica*, **A64**, 112–122.

Shen, J. and Moore, P.B. (1982) Törnebohmite, $RE_2Al(OH)[SiO_4]_2$: crystal structure and genealogy of RE(III)Si(IV) ↔ Ca(II)P(V) isomorphisms. *American Mineralogist*, **67**, 1021–1028.

Spek, A.L. (2009) Structure validation in chemical crystallography. *Acta Crystallographica*, **D65**, 148–155.

Spencer, L.J. (1913) A (sixth) list of new mineral names.

Mineralogical Magazine, **16**, 352–378.

Strunz, H. and Nickel, E.H. (2001) *Strunz Mineralogical Tables. Chemical Structural Mineral Classification System*, 9th Edition. Schweizerbart, Stuttgart, Germany, 870 pp.

Twarakavi, N.K.C. and Kaluarachchi, J.J. (2006) Arsenic in the shallow ground waters of conterminous United States: assessment, health risks, and costs for MCL compliance. *Journal of American Water Resources Association*, **42**, 275–294.

Vaughan, D.J. (2006) Arsenic. *Elements*, **2**, 71–75.

Vésignié, J.P.L. (1935) Présentation d'échantillons. *Bulletin de la Société française de Minéralogie*, **58**, 4–5 [in French].

Walenta, K. and Dunn, P.J. (1984) Arsenogoyazit, ein neues mineral der crandallitgruppe aus dem Schwarzwald. *Schweizerische Mineralogische und Petrographische Mitteilungen*, **64**, 11–19 [in German].

Wherry, E.T. (1921) New minerals. *American Mineralogist*, **6**, 118–119.

Williams, S.A. (1973) Heyite, $Pb_5Fe_2(VO_4)_2O_4$, a new mineral from Nevada. *Mineralogical Magazine*, **39**, 65–68.

Wilson, A.J.C. (editor) (1992) *International Tables for Crystallography. Volume C: Mathematical, physical and chemical tables*. Kluwer Academic Publishers, Dordrecht, The Netherlands.

Wojdyr, M. (2010) *Fityk*: a general-purpose peak fitting program. *Journal of Applied Crystallography*, **43**, 1126–1128.

Yakubovich, O.V., Massa, W. and Pekov, I.V. (2002) Crystal structure of the new mineral bushmakinite, $Pb_2\{(Al,Cu)[PO_4][(V,Cr,P)O_4](OH)\}$. *Doklady Earth Sciences*, **382**, 100–105.

Zubkova, N.V., Pushcharovsky, D.Y., Giester, G., Tillmanns, E., Pekov, I.V. and Kleimenov, D.A. (2002) The crystal structure of arsentsumebite, $Pb_2Cu[(As,S)O_4]_2(OH)$. *Mineralogy and Petrology*, **75**, 79–88.